IOP PUBLISHING JOURNAL OF OPTICS
J. Opt. **15** (2013) 044024 (5pp) doi:10.1088/2040-8978/15/4/044024

Circular lines of circular polarization in three dimensions, and their transverse-field counterparts

M V Berry

H H Wills Physics Laboratory, Tyndall Avenue, Bristol BS8 1TL, UK

E-mail: asymptotico@physics.bristol.ac.uk

Received 28 December 2012, accepted for publication 30 January 2013
Published 10 April 2013
Online at stacks.iop.org/JOpt/15/044024

Abstract
A superficially paradoxical phenomenon is associated with curved c lines, on which the polarization of a three-dimensional optical field in space is purely circular. If the c line has fixed index (signed half-integer winding number), its two intersections with an observation plane, each with the same index, coalesce and annihilate when the c line is tangent to the plane, seeming to contradict the conservation of index. But there is no paradox: for the associated C line (distinct from the c line) on which the field transverse to the observation plane is circularly polarized, the two intersections have opposite indices, so their total index is zero, which is conserved during the annihilation. The different geometries of the c and C lines are studied in detail for model fields where the c line is a circle.

Keywords: singularities, electromagnetism, topology

1. Introduction

Much insight into monochromatic optical fields in three dimensions has followed the identification by Nye and Hajnal [1–5] of lines on which the light is circularly polarized: that is, the polarization ellipse is a circle. The characterization of these polarization singularities includes their index: the number of times the polarization ellipse (almost circular near the line) rotates during a circuit of the line. The index is $S = \pm 1/2$. For $S = -1/2$, there is one pattern of almost-circular ellipses: the star; for $S = +1/2$ there are two: the lemon and the monstar [2, 6].

The singular lines can be defined in two ways. The first, and more fundamental, are c lines, corresponding to circular polarization of the full three-dimensional field. The second is relevant to fields where a particular direction is identified, for example perpendicular to observation planes in paraxial optics; then the corresponding transverse fields also possess lines of circular polarization, namely the C lines (figure 1). (This terminology differs from that originally introduced [1], in which what we call c lines were called C^T lines, the T denoting 'true'. We avoid this because of possible confusion between 'true' and its opposite in this context, namely 'transverse'. It also differs from terminology I regrettably introduced earlier [7], in which c and C have the opposite meanings to those I now prefer.)

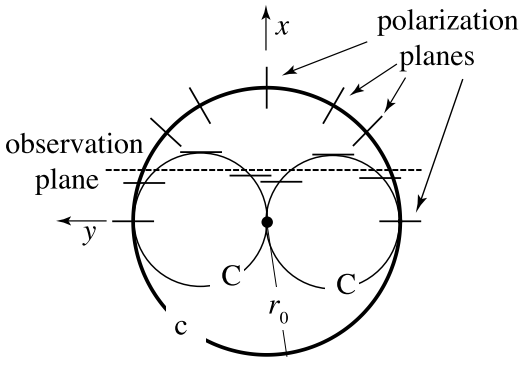

Figure 1. Circular c line, and associated C line for observation planes labelled by x (one shown dashed), and corresponding polarization planes.

In general, c and C lines are different from each other and also for the electric and magnetic parts of the optical field. For paraxial fields in which these lines are nearly parallel to the

propagation direction, the four lines are close to each other, in ways that are understood [7]. My aim here is to illustrate, for the electric field, the opposite situation, in which the c and C lines bend through large angles and have very different geometries, and to dissolve an apparent paradox.

Along a c line, the orientation of the polarization circle usually changes. If the normal to the circle is perpendicular to the c line at some point—that is, if the c line is tangent to the circle—the index switches sign [1, 8]. The emphasis here is on the situation in which this switch never occurs. An extreme is when the circle is always perpendicular to the c line, that is, where the normal to the circle coincides with the c line and turns rigidly with it as the c line bends. If an observation plane is translated perpendicular to itself (figure 1) so that two intersections of a curved c line coalesce (when the c line is tangent to the plane) and then annihilate, this corresponds to the disappearance of two singularities with the same index, apparently violating index conservation.

To dispel the paradox, it is helpful to begin with an analogy. Instead of optics, regard the c line as a uniform curved thin wire, whose intersections with the plane represent a pair of 'masses'. The coalescence and disappearance of these masses does not contradict the conservation of mass. In the optical case, the appearance of paradox arises from a failure to distinguish c and C lines. Where a C line is tangent to the observation plane, the associated index (of the transverse field) does switch sign. Starting from a situation in which the c and C lines coincide, for example where both are perpendicular to an observation plane, and then translating the plane so it is no longer perpendicular to the c line, the c and C lines separate. The location of the plane where it is tangent to the c line is different from the location where it is tangent to the C line.

To illustrate this phenomenon, a class of divergenceless electric fields will be constructed (section 2) whose c lines are circles, an explicit example being explored analytically in section 3. The corresponding very different C lines are described in section 4.

2. General theory for circular c lines and C lines

Using cylindrical polar coordinates in three-dimensional space, we create complex electric fields with a circular c line in the plane $z = 0$, centred on the origin $r = 0$ and with radius r_0, polarized in the plane perpendicular to azimuthal direction ϕ, that is

$$\boldsymbol{E}(\boldsymbol{r}) = E_r(r, z)\boldsymbol{e}_r + E_z(r, z)\boldsymbol{e}_z. \tag{2.1}$$

To ensure divergencelessness, each such field will be derived from an azimuthally directed vector potential:

$$\boldsymbol{E}(\boldsymbol{r}) = \nabla \times (A(r, z)\boldsymbol{e}_\phi). \tag{2.2}$$

Thus

$$E_r(r, z) = -\partial_z A(r, z), \qquad E_z(r, z) = \frac{1}{r}\partial_r(rA(r, z)). \tag{2.3}$$

All c lines of the field $\boldsymbol{E}$ correspond to nodal lines of an associated complex scalar field $\psi(\boldsymbol{r})$, that is, they are phase vortices of $\psi(\boldsymbol{r})$ (whose phase gradient is unrelated to the Poynting vector of the optical field):

$$\psi(\boldsymbol{r}) = \boldsymbol{E}(\boldsymbol{r}) \cdot \boldsymbol{E}(\boldsymbol{r}) = E_r^2(r, z) + E_z^2(r, z) = 0. \tag{2.4}$$

The desired c line, with a convenient normalization, can be fixed by the requirement

$$E_r(r_0, 0) = 1, \qquad E_z(r_0, 0) = \mathrm{i}. \tag{2.5}$$

In sections 3 and 4 we will study a class of low-order polynomial fields with the convenient property that the c and C lines can be calculated analytically. These model fields do not satisfy Maxwell's equations, but it is easy to generate ones that do, that is, fields for which, with wavenumber k,

$$(\nabla^2 + k^2)A(r, z)\boldsymbol{e}_\phi = 0. \tag{2.6}$$

The general solution is

$$A(r, z) = \sum_{q,+,-} c_\pm(q)J_1(qr)\exp(\pm \mathrm{i}z\sqrt{k^2 - q^2}), \tag{2.7}$$

representing a superposition of vector Bessel beams with transverse wavenumbers q (which can be arbitrary complex numbers) and waves travelling in the $\pm z$ directions. The corresponding electric field components are

$$\begin{aligned} E_r(r, z) &= \mathrm{i}\sum_{q,+,-} \pm\sqrt{k^2 - q^2}c_\pm(q) \\ &\quad \times J_1(qr)\exp(\pm \mathrm{i}z\sqrt{k^2 - q^2}) \\ E_z(r, z) &= \sum_{q,+,-} qc_\pm(q)J_0(qr)\exp(\pm \mathrm{i}z\sqrt{k^2 - q^2}). \end{aligned} \tag{2.8}$$

Numerical exploration of some simple cases, for example

$$A(r, z) = cJ_1(qr)\exp(\mathrm{i}z\sqrt{k^2 - q^2}) + dJ_1(kr), \tag{2.9}$$

indicates that the c and C line structures resemble those in the polynomial model of sections 3 and 4. Further study of more general superpositions would be worthwhile.

For the related transverse fields, we consider observation planes with constant x. Thus

$$\begin{aligned} \boldsymbol{E}_{\mathrm{trans}}(\boldsymbol{r}) &= E_y(\boldsymbol{r})\boldsymbol{e}_y + E_z(\boldsymbol{r})\boldsymbol{e}_z \\ &= E_r(\sqrt{x^2 + y^2}, z)\frac{y}{\sqrt{x^2 + y^2}}\boldsymbol{e}_y \\ &\quad + E_z(\sqrt{x^2 + y^2}, z)\boldsymbol{e}_z. \end{aligned} \tag{2.10}$$

The corresponding C lines are determined by

$$\begin{aligned} \psi_{\mathrm{trans}}(\boldsymbol{r}) &= \boldsymbol{E}_{\mathrm{trans}}(\boldsymbol{r}) \cdot \boldsymbol{E}_{\mathrm{trans}}(\boldsymbol{r}) \\ &= E_y^2 + E_z^2 = E_r^2\frac{y^2}{r^2} + E_z^2 = 0. \end{aligned} \tag{2.11}$$

Because the orientation of the observation plane breaks rotational symmetry, these C lines will generally not be circles centred on the origin.

Although we will be concerned with the electric c and C lines, it is worth noting that the associated magnetic fields display very different behaviour. From Maxwell's equations,

$$B(\boldsymbol{r}) = -\frac{\mathrm{i}}{ck}\nabla \times \boldsymbol{E}(\boldsymbol{r}) = -\frac{\mathrm{i}}{ck}(\partial_z E_r - \partial_r E_z)\boldsymbol{e}_\phi. \tag{2.12}$$

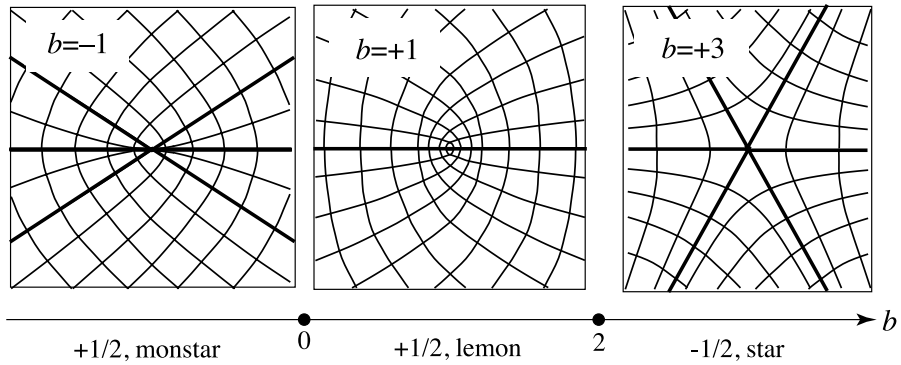

Figure 2. Polarization patterns (streamlines of ellipse principal axis directions) and singularity indices for c line associated with the field (3.2), for different ranges of the parameter b. The patterns are calculated on squares with side length 0.4 centred on the c line.

This represents a linearly polarized field—that is, a field with no c or C lines—a vortex circulating round the z axis, illustrating in a dramatic way the known fact [1, 2] that the singularity structure of the electric and magnetic fields can be very different.

3. c lines for model three-dimensional fields

The model divergenceless electric field to be explored, constructed to have a c line with $r_0 = 1$, is based on the vector potential in (2.2), where

$$A(r, z) = \tfrac{1}{4}\mathrm{i}r^3 - rz(1 + \tfrac{1}{2}\mathrm{i}bz). \tag{3.1}$$

The divergenceless field thus generated is

$$\begin{aligned}\boldsymbol{E}(\boldsymbol{r}) &= r(1 + \mathrm{i}bz)\boldsymbol{e}_r + (-2z + \mathrm{i}(r^2 - bz^2))\boldsymbol{e}_z \\ &= (1 + \mathrm{i}bz)(x\boldsymbol{e}_x + y\boldsymbol{e}_y) + (-2z + \mathrm{i}(r^2 - bz^2))\boldsymbol{e}_z.\end{aligned} \tag{3.2}$$

As will be shown, different ranges of the parameter b represent fields with c lines of star, monstar and lemon type.

The condition (2.4) for a c singularity has three solutions:

$$\begin{aligned} &r = 1, && z = 0 && \text{(c1)} \\ &r = \frac{2}{b}, && z = \pm\sqrt{\frac{2(2-b)}{b^3}} && \text{(c2)} \\ &r = 0, && z = 0 && \text{(c3)}. \end{aligned} \tag{3.3}$$

Solution (c1) is the one of principal interest. As described in the appendix, standard formulae [2, 9] imply that this c circle of unit radius has the local geometry, depending on b, illustrated in figure 2. (With the single parameter b, the patterns are symmetric, and this suffices for present purposes; the full unsymmetric unfoldings of c singularities would require an additional parameter [6].)

The solution (c2), which exists only for $0 < b < 2$, is a pair of rings each with index $-1/2$ and so of star type. Thus

$$S_{\mathrm{c1}} = \tfrac{1}{2}\mathrm{sgn}(2 - b), \qquad S_{\mathrm{c2}} = \tfrac{1}{2}\mathrm{sgn}(b - 2) = -\tfrac{1}{2}. \tag{3.4}$$

The solution (c3) is a field nodal point of saddle type, where the field is locally real, that is

$$\boldsymbol{E}(\boldsymbol{r}) \approx x\boldsymbol{e}_x + y\boldsymbol{e}_y - 2z\boldsymbol{e}_z. \tag{3.5}$$

Such a singular point is non-generic for electric fields in three dimensions, and occurs here as a result of symmetry; it is irrelevant to the c and C behaviour we are studying. To be noted, however, is that the c circle (or three c circles if $0 < b < 2$), are threaded by the z axis on which the vorticity $\boldsymbol{\omega}(\boldsymbol{r})$ of the associated scalar field $\psi(\boldsymbol{r})$ vanishes; the z axis is a vortex line of the vorticity

$$\begin{aligned}\boldsymbol{\omega}(\boldsymbol{r}) &= \mathrm{Im}[\nabla\psi^*(\boldsymbol{r}) \times \nabla\psi(\boldsymbol{r})] = 2\,\mathrm{Im}[\partial_z\psi^*\partial_r\psi]\boldsymbol{e}_\phi \\ &\underset{r\to 0}{\to} 8rz^2(b - 8)\boldsymbol{e}_\phi.\end{aligned} \tag{3.6}$$

For the magnetic field corresponding to (3.2) and (2.11) gives

$$\boldsymbol{B} = \frac{1}{ck}r(b - 2)\boldsymbol{e}_\phi. \tag{3.7}$$

4. C line for transverse model fields

The transverse field corresponding to (3.2), for observation planes labelled by x, is

$$\boldsymbol{E}_{\mathrm{trans}}(\boldsymbol{r}) = (1 + \mathrm{i}bz)y\boldsymbol{e}_y + (-2z + \mathrm{i}(x^2 + y^2 - bz^2))\boldsymbol{e}_z. \tag{4.1}$$

The corresponding C lines, determined by (2.10) and illustrated in figure 3 together with the c circles, are

$$\begin{aligned} &z = 0, \quad r^2 = |y|, && \text{i.e. } z = 0, \\ &\qquad y = \pm\tfrac{1}{2} \pm \sqrt{x^2 - \tfrac{1}{4}} && \text{(C1)} \\ &z = \pm\sqrt{\frac{x^2b^2 - (2b - 4)}{b^3}}, && y = \pm\frac{2}{b}. \quad \text{(C2)} \end{aligned} \tag{4.2}$$

For all b, the C1 lines are two circles inscribed in the main c circle and touching at $r = z = 0$. The C2 lines exist for $b > 0$, and are hyperbolas, separate from the pairs of circles C1 if $0 < b < 2$, and intersecting them if $b > 2$.

For the indices, a calculation described in the appendix gives

$$\begin{aligned} S_{\mathrm{C1}} &= \tfrac{1}{2}\mathrm{sgn}[(1 - 2|y|)(b|y| - 2)] \\ S_{\mathrm{C2}} &= -\tfrac{1}{2}\mathrm{sgn}[(4 - 2b + b^2x^2)(4 - b + b^2x^2)]. \end{aligned} \tag{4.3}$$

These are illustrated in figure 4. The c and C indices coincide at $y = \pm 1$, where the c and C lines touch. The C indices on

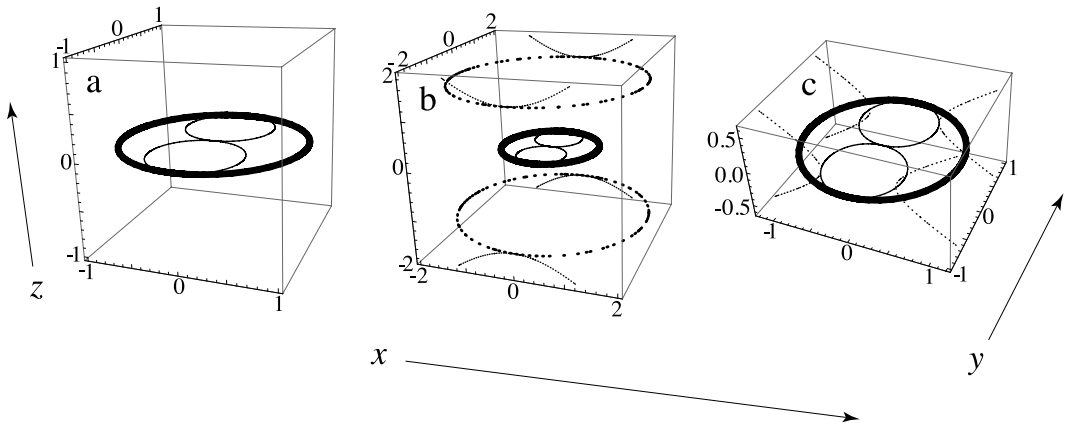

Figure 3. Circular polarization lines for the field (3.2), for (a) $b = -1$, (b) $b = +1$, (c) $b = +3$. Thick curve: unit c circle ((c1) in (3.3)); thick dots: c circles (c2) in (3.1); thin curves: C circles C1 in (4.2); thin dotted hyperbolas: C lines C2 in (4.2).

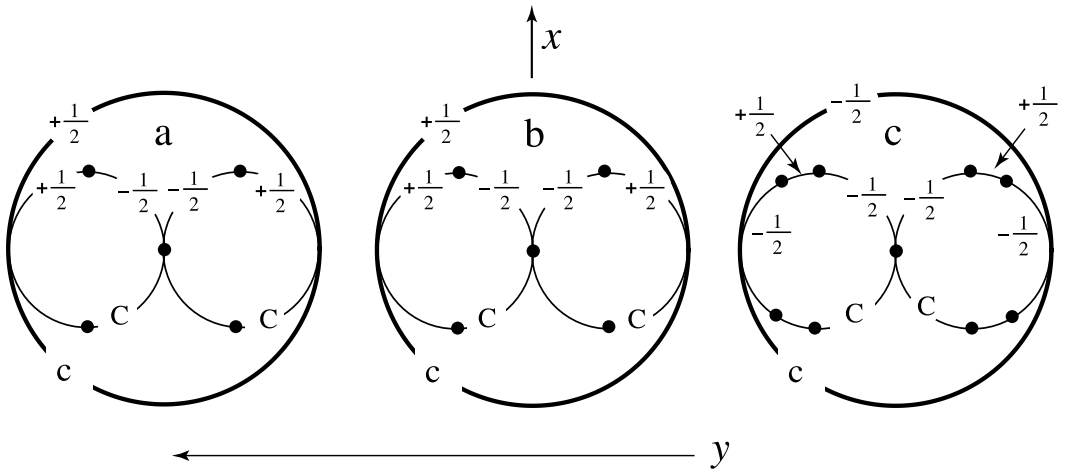

Figure 4. Indices for the c circle and the C circles that touch it, for (a) $b = -1$; (b) $b = +1$; (c) $b = +3$. Black dots indicate places on the C line where the index switches. (The pictures (b) and (c) are the same.)

the two C1 circles switch at $x = y = \pm 1/2$ where the C line touches the observation plane and two C singularity points in the plane coalesce. In addition, for $b > 2$ there are switch points at $y = \pm 2/b$ where the C1 type C lines and the C2 type C lines intersect (see figure 3(c)).

5. Concluding remarks

c lines are more fundamental than C lines, because their definition is independent of the choice of observation planes. But the C lines are easier to observe, because they depend only on the transverse fields. This discordance was the motivation for the study reported here. Using the model field (3.2) and its transverse counterpart (4.1), the separation of c and C lines has been explored in detail. But the phenomenon is not restricted to simple models: it is general, associated with any curved c line, because a series of observation planes can always be chosen such that one of them becomes tangent to the c line at any chosen point on it.

The phenomenon can occur in paraxial fields. An example is the superposition (2.7) with all $q \ll k$; circular c lines can easily be constructed by the prescription (2.5). But note that such c circles are perpendicular to the paraxial direction $\boldsymbol{e}_z$, and the observation planes for which the C lines differ radically from the c lines are labelled by x or y, rather than z (which is the more familiar situation in which c and C lines nearly coincide [7]).

Finally, it is worth noting a partial analogy between the polarization phenomenon studied here and a feature identified [10–12] for curved vortex lines in complex scalar fields. As an observation plane is translated so as to become tangent to a vortex line, two intersections coalesce and annihilate; they have opposite indices relative to the normal to the observation plane, but the index relative to the direction of the vortex line is preserved. This apparent discordance of indices is analogous to that for c and C singularities. A unifying feature is that for scalar vortex lines and c and C lines the sense of the vorticity $\boldsymbol{\omega}(\boldsymbol{r})$, defined by the second equation in (A.1) with the appropriate complex scalar $\psi(\boldsymbol{r})$, is conserved along the lines as they curve, even in cases where the index switches between $+1/2$ and $-1/2$. The difference between the cases is that there is only one vortex line, but there are the two separate c and C circular polarization lines.

Acknowledgments

This work was stimulated by a question from Professor Marat Soskin, for which I thank him. I also thank Dr Mark Dennis for his helpful comments. Generous hospitality during this research was provided by the Isaac Newton Institute, Cambridge, and the Indian Institute for Science Education and Research, Kolkata. My research is supported by the Leverhulme Trust.

Appendix. Index calculations

The index S of a c line at a point $\boldsymbol{r}$ is known [9] to be half the sign of the component of the normal $\boldsymbol{N}(\boldsymbol{r})$ to the polarization circle along the direction of the c line, which is the vorticity $\boldsymbol{\omega}(\boldsymbol{r})$ of the associated scalar field $\psi(\boldsymbol{r})$ defined by (2.4). Using

$$\boldsymbol{N} = \mathrm{Im}\,\boldsymbol{E}^* \times \boldsymbol{E}, \qquad \boldsymbol{\omega} = \mathrm{Im}\nabla\psi^* \times \nabla\psi, \tag{A.1}$$

gives, for the field (2.1),

$$S = \tfrac{1}{2}\boldsymbol{N}\cdot\boldsymbol{\omega} = \tfrac{1}{2}\mathrm{sgn}[\mathrm{Im}\,E_z^* E_r\ \mathrm{Im}\,\partial_z\psi^*\partial_r\psi]. \tag{A.2}$$

Direct application of this formula gives the indices (3.4) for the c circles of the model field (3.2).

Where $S = -1/2$, the c line is of star type. Where $S = +1/2$, there are two possibilities to be distinguished in the pattern of ellipse principal axes in planes near the singularity: lemon, for which there is one locally straight line of each principal axis direction through the point where the c line intersects a plane, and monstar, for which there are three. The criterion for a straight line through the c point is that the direction $\theta(\phi)$ of a principal axis at points with azimuth ϕ coincides with ϕ.

It will suffice to consider the major axis, whose direction [9] is

$$\boldsymbol{E}_+(\boldsymbol{r}) \propto \mathrm{Re}[\boldsymbol{E}^*(\boldsymbol{r})\sqrt{\psi(\boldsymbol{r})}]. \tag{A.3}$$

For the c line (2.5), and if the phase of the ψ vortex is $\gamma(\phi)$, i.e.

$$\psi = |\psi(\phi)|\exp(\mathrm{i}\gamma(\phi)), \tag{A.4}$$

equation (A.3) gives

$$\boldsymbol{E}_+(\boldsymbol{r}) = \left\{\cos\tfrac{1}{2}\gamma(\phi), \sin\tfrac{1}{2}\gamma(\phi)\right\}. \tag{A.5}$$

Thus $\theta(\phi) = \gamma(\phi)/2$, and the condition $\theta(\phi) = \phi$ gives

$$\tan 2\phi = \tan\gamma(\phi). \tag{A.6}$$

Near the c intersection point, ψ is a locally linear function of the local Cartesian coordinates, so

$$\psi(\phi) \approx u\cos\phi + v\sin\phi, \tag{A.7}$$

where the constant coefficients u and v are complex. Thus the phase in (A.4) is given by

$$\tan\gamma(\phi) = \frac{\mathrm{Im}\,u + \mathrm{Im}\,v\tan\phi}{\mathrm{Re}\,u + \mathrm{Re}\,v\tan\phi}. \tag{A.8}$$

Now (A.6) can be reduced to a cubic equation for $\tan\phi$, whose discriminant [2, 6] determines whether there are three solutions (monstar) or one (lemon). When applied to the field (3.2), these arguments give the patterns in figure 2.

The calculations are very similar for the C lines. Instead of (A.2), the index for the transverse field (4.1) is

$$S_{\mathrm{trans}} = \tfrac{1}{2}\mathrm{sgn}[\mathrm{Im}\,E^*_{\mathrm{trans}\ y}E^*_{\mathrm{trans}\ z}\mathrm{Im}\,\partial_y\psi^*_{\mathrm{trans}}\partial_z\psi_{\mathrm{trans}}]. \tag{A.9}$$

Direct application leads to the indices (4.3), as indicated in figure 4.

References

[1] Nye J F and Hajnal J V 1987 The wave structure of monochromatic electromagnetic radiation *Proc. R. Soc.* A **409** 21–36
[2] Nye J F 1999 *Natural Focusing and Fine Structure of Light: Caustics and Wave Dislocations* (Bristol: Institute of Physics Publishing)
[3] Hajnal J V 1987 Singularities of the transverse fields of electromagnetic waves. I. Theory *Proc. R. Soc.* A **414** 433–46
[4] Hajnal J V 1987 Singularities in the transverse fields of electromagnetic waves. II. Observations on the electric field *Proc. R. Soc.* A **414** 447–68
[5] Hajnal J V 1990 Observation of singularities in the electric and magnetic fields of freely propagating microwaves *Proc. R. Soc.* A **430** 413–21
[6] Dennis M R 2008 Polarization singularity anisotropy: determining monstardom *Opt. Lett.* **33** 2572–4
[7] Berry M V 2004 The electric and magnetic polarization singularities of paraxial waves *J. Opt.* A **6** 475–81
[8] Flossman F, O'Holleran K, Dennis M R and Padgett M J 2008 Polarization singularities in 2D and 3D speckle fields *Phys. Rev. Lett.* **100** 203902
[9] Berry M V 2004 Index formulae for singular lines of polarization *J. Opt.* A **6** 675–8
[10] Berry M V 1998 Much ado about nothing: optical dislocation lines (phase singularities, zeros, vortices...) *Proc. SPIE* **3487** 1–5
[11] Freund I 2001 Critical foliations and Berry's paradox *Opt. Photon. News* **12** 56
[12] Freund I 2000 Optical vortex trajectories *Opt. Commun.* **181** 19–33